ChemBioChem

Research Article
doi.org/10.1002/cbic.202400187

Chemistry Europe
European Chemical Societies Publishing

www.chembiochem.org

Proteomic Profiling of Antimalarial Plasmodione Using 3-Benz(o)ylmenadione Affinity-Based Probes

Ilaria Iacobucci[+],[a, b, c] Vittoria Monaco[+],[a, b, c] Agnès Hovasse,[b] Baptiste Dupouy,[a] Rodrigue Keumoe,[d] Bogdan Cichocki,[a] Mourad Elhabiri,[a] Brigitte Meunier,[e] Jean-Marc Strub,[b] Maria Monti,[c] Sarah Cianférani,[b] Stéphanie A. Blandin,[d] Christine Schaeffer-Reiss,[b] and Elisabeth Davioud-Charvet*[a]

Understanding the mechanisms of drug action in malarial parasites is crucial for the development of new drugs to combat infection and to counteract drug resistance. Proteomics is a widely used approach to study host-pathogen systems and to identify drug protein targets. Plasmodione is an antiplasmodial early-lead drug exerting potent activities against young asexual and sexual blood stages in vitro with low toxicity to host cells. To elucidate its molecular mechanisms, an affinity-based protein profiling (AfBPP) approach was applied to yeast and *P. falciparum* proteomes. New (*pro*-) AfBPP probes based on the 3-benz(o)yl-6-fluoro-menadione scaffold were synthesized. With optimized conditions of both photoaffinity labeling and click reaction steps, the AfBPP protocol was then applied to a yeast proteome, yielding 11 putative drug-protein targets. Among these, we found four proteins associated with oxidoreductase activities, the hypothesized type of targets for plasmodione and its metabolites, and other proteins associated with the mitochondria. In *Plasmodium* parasites, the MS analysis revealed 44 potential plasmodione targets that need to be validated in further studies. Finally, the localization of a 3-benzyl-6-fluoro-menadione AfBPP probe was studied in the subcellular structures of the parasite at the trophozoite stage.

Introduction

Functional proteomics is devoted to the elucidation of molecular mechanisms in living cells through the investigation of biomolecule interactions. Several approaches have been developed over the years depending on the nature of the interactions and the biomolecules involved,[1,2] leading to the establishment of specific branches of chemistry, such as chemical biology. In particular, chemical proteomics has emerged as a powerful tool to study the interactions between small molecules and proteins.[3,4] In this context, one of the approaches used to identify molecular or drug targets is affinity-based protein profiling (ABPP), a method pioneered by Cravatt and others.[5–8]

This approach, increasingly employed for target identification in malarial parasites, consists in using 'clickable' covalent inhibitor-based probes (ABPP probes)[9,10] or affinity-based photoactivatable and 'clickable' probes (AfBPP probes)[11] to facilitate chemical pulldowns of the probe-protein adducts. AfBPP probes contain both a photo-affinity group and a reporter group for bioorthogonal chemistry (typically an alkyne), which are attached to a compound of interest at a tolerant position. Live cells or extracted proteins from cell lysates are incubated with AfBPP probes and irradiated with UV light. UV exposure triggers the photolabeling reactive moiety to

[a] *Dr. I. Iacobucci,[+] V. Monaco,[+] B. Dupouy, Dr. B. Cichocki, Dr. M. Elhabiri, Dr. E. Davioud-Charvet*
Laboratoire d'Innovation Moléculaire et Applications (LIMA), Team Bio(IN)-organic & Medicinal Chemistry,
UMR7042 CNRS-Université de Strasbourg-Université Haute-Alsace
European School of Chemistry, Polymers and Materials (ECPM), 25, rue Becquerel, 25, rue Becquerel, F-67087 Strasbourg (France)
E-mail: elisabeth.davioud@unistra.fr

[b] *Dr. I. Iacobucci,[+] V. Monaco,[+] Dr. A. Hovasse, Dr. J.-M. Strub, Dr. S. Cianférani, Dr. C. Schaeffer-Reiss*
Laboratoire de Spectrométrie de Masse BioOrganique
IPHC UMR 7178 CNRS, Université de Strasbourg, 67087 Strasbourg (France) and
Infrastructure Nationale de Protéomique ProFI – FR2048, F-67087 Strasbourg, (France)

[c] *Dr. I. Iacobucci,[+] V. Monaco,[+] Prof. M. Monti*
Department of Chemical Sciences
University of Naples Federico II
Complesso Universitario di Monte Sant' Angelo, Via Cintia 26, I-80126 Napoli (Italy)

[d] *Dr. R. Keumoe, Dr. S. A. Blandin*
Institut de Biologie Moléculaire et Cellulaire,
INSERM U1257 – CNRS UPR9022 – Université de Strasbourg,
2, Allée Konrad Roentgen-67084, Strasbourg (France)

[e] *Dr. B. Meunier*
Institute for Integrative Biology of the Cell (I2BC),
CEA, CNRS, Univ. Paris-Sud, Université Paris-Saclay,
91198 Gif-Sur-Yvette Cedex, France

[+] *Authors contributed equally as first co-authors*

Supporting information for this article is available on the WWW under https://doi.org/10.1002/cbic.202400187

form a covalent adduct with the protein target. Then, the 'clickable' reporter tag (alkyne) ensures the labeling of the protein-probe adduct (s) by copper (I)-catalyzed alkyne-azide cycloaddition (CuAAC) "click" reaction with an azide partner (e.g. biotin azide) used for enrichment (e.g. on avidin beads). The labeling step through the biotinylation reaction is required to purify the adducts by affinity-based strategies.[12]

Malaria is the most devastating tropical parasitic disease causing 619,000 deaths/year. It is both a cause and a consequence of poverty, mostly in Sub-Saharan Africa, by impacting social and economic lives. The limited arsenal of effective and nontoxic drugs to cure this devastating infectious disease and their inefficacy to kill resistant parasites, represent major public health challenges. The launching of new generation of antimalarial drugs active against artemisinin-resistant parasites and blocking transmission of the parasites to the mosquitoes would represent a big hope towards malaria control and elimination. The widespread development of drug-resistant parasite strains against the commonly used drug series of endoperoxides, illustrated by the lead drug artemisinin, creates a necessity to identify new drug targets and to develop original chemotypes with new modes of action (MoA). Open access to the full *Plasmodium* genome and proteome has brought new opportunities to identify novel drug targets. So far, very few oxidoreductases have been identified as antimalarial drug targets.[13,14]

In the last decade, we have discovered an early lead redox-active compound, called plasmodione (**PD**), belonging to the 3-benzylmenadione (benzylMD) family, with a unique mechanism of action[15] that has been partly deciphered (Figure 1, panel A). **PD** acts as a prodrug entering in a cascade of redox reactions, with highest activity in young early stages and gametocytes.[16] Its specific bioactivation generates a key 3-benzoylmenadione (benzoylMD) called plasmodione oxide (**PDO**) with increased oxidant properties.[17] The active metabolite $\mathbf{PDO_{ox}}$ was shown to act as a subversive substrate of various flavoenzymes, producing reduced **PDO** ($\mathbf{PDO_{red}}$) and initiating a redox-cycling process in the presence of oxygen or methemoglobin. This redox cycling produces damaging compounds such as the benzoxanthone (**BX**),[18] reactive oxygen species (ROS) and oxidative stress, and finally leads to parasite death. Through its key metabolite $\mathbf{PDO_{ox}}$, **PD** likely interacts with several oxidoreductases, associated with multiple vital processes of *P. falciparum*-parasitized red blood cells (pRBCs).

Recently, we designed innovative (*pro*-) AfBPP probes, based on the benzylMD skeleton, as prodrugs entering a cascade of photoredox-reactions to generate related AfBPP probes with a benzophenone-like structure, as found in $\mathbf{PDO_{red}}$.[19] The benzylMD core was photoreduced and then oxidized at the benzylic chain under UV irradiation.[20] The generated reduced benzoylMD covalently reacted with target proteins under UV irradiation. The probe-protein adducts were then clicked with biotin-PEG3-azide (BA) using the CuAAC reaction, pulled-down, digested and analyzed by LC–MS/MS. The AfBPP strategy has been successfully applied to recombinant glutathione reductases from the pRBC unit. Noteworthy, we used 3-benzylMD as (*pro*-) AfBPP probes for the following reasons: i) the released benzophenone-like unit is stable and can be generated in a cascade of redox-reactions catalyzed by oxidoreductases, as **PDO** is generated from **PD**;[20] ii) under high-energy excitation wavelength (350 nm), benzyl MDs can also be activated in benzoylMDs;[20] iii) the UV-light generated excited diradicaloid triplet species (benzophenone-like moiety) reacts preferentially with C–H bonds in the presence of water or other nucleophiles[21] and iv) if no C–H bond is available, the short-lived diradical species can then relax back to the ground state and reinstate the oxidized benzoylMD, rendering the excitation of the probe reversible in favor of specific labeling.[22]

The AfBPP probes used in the present work are shown in Figure 1, panel B. In particular, the former probes **1** and **2**[19] were used here to optimize the click reaction by employing tetrakis (acetonitrile) copper (I) instead of copper (II) sulfate. Regarding the photoaffinity labelling reaction, as we started from a low yield (5%), we designed and synthesized the new probe **3**, with a fluorine atom at C-6 (Figure 1B), with the aim of enhancing the photoreduction kinetics and increasing the yield of the photoalkylation reaction at the carbonyl group. Since yeast is sensitive to **PD** activity, we used it as a model system to test the whole optimized pipeline both in term of UV irradiation and click reaction conditions. In *S. cerevisiae* cell lysates where bioactivation may not occur, we used the new benzoylMD probe **3** in the AfBPP experiments. In addition, we incubated live *P. falciparum*-pRBCs with the novel (*pro*-) AfBPP probe **5** (Figure 1B), and applied the AfBPP workflow (UV irradiation + click reaction, Figure 1C) on cell lysates. The AfBPP strategy in yeast and *Plasmodium falciparum* revealed potential PD targets that need to be validated in further studies.

Results and Discussion

Following our seminal work with pure recombinant proteins,[19] we improved the (*pro*-) AfBPP methodology by optimizing both the yields of the photoirradiation and the click reaction (CuAAC) using previously reported and new probes and different read-outs. We explored the possibility to do so in SDS-PAGE gels using a fluorophore coupled with an azide. However, we demonstrated that a CuAAC-independent fluorescence signal associated to **PDO**-protein adducts was produced by an Excited State Intramolecular Photoinduced Transfer (ESIPT) mechanism,[23] which precluded its use for this specific purpose (See supporting information, section B2.1 including Figures S1–S4).

Optimization of the Click Conditions in Aqueous Solutions

The optimization of the click reaction in quasi-physiological aqueous milieu and the setting up of the best conditions compatible with the proteomics pipeline are critical parameters to improve the whole AfBPP workflow yield. Starting from our reported conditions (i.e. 55% yield with a rhodamine-based fluorophore azide),[19] we first optimized the CuAAC yield using probe **1** and BA (See supporting information, Table S1, Figur-

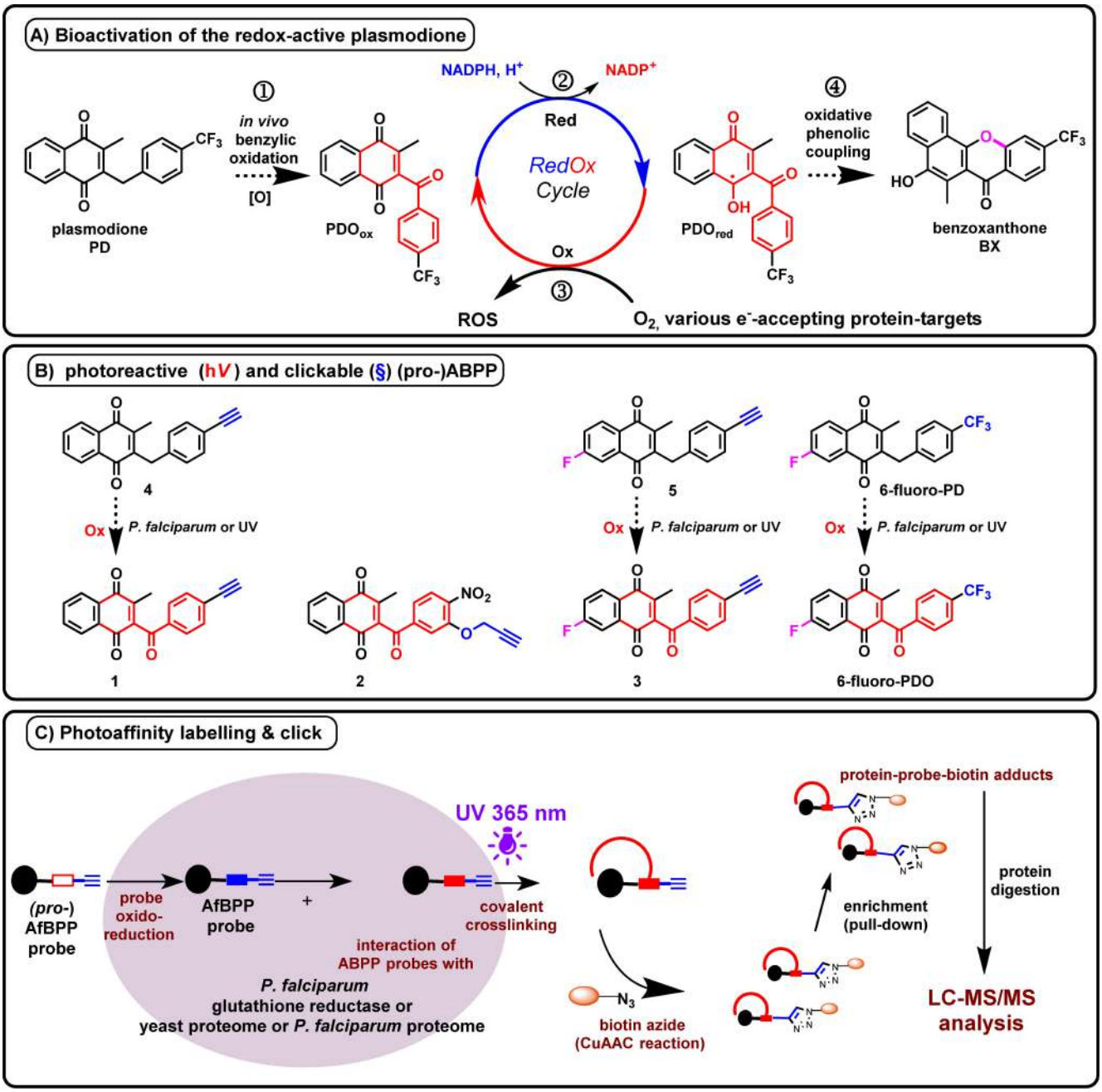

Figure 1. (A) Bioactivation of Plasmodione (**PD**): upon internalization in the parasite, plasmodione **PD** is proposed to generate **PDO$_{ox}$**, a drug metabolite, by benzylic oxidation (step 1), the 3-benzoylmenadione (benzoylMD), which, under its oxidized form, possesses a photoreactive benzophenone-like moiety (indicated in red). This metabolite is further reduced (step 2), and **PDO$_{red}$** takes part in oxidoreductase-mediated redox-cycling (step 3) leading to ROS-induced parasite death. (B) Plasmodione-affinity based probes (PD-AfBPP): The common scaffold of the PD-AfBPP probes **1**–**3** and **6-fluoro-PDO** is a photoreactive benzoylMD, functionalized by different electron-withdrawing groups in *para* position of the benzylic chain (–CF_3 or -alkyne), and a H or F at C-6 of the menadione core, affecting their photoreactivity. Introduction of the fluorine atom at C-6 of the menadione core was designed to improve the efficiency of the AfBPP probe. The parent benzylMDs, the (*pro*-) AfBPP probes **5**–**6** or the **6-fluoro-PD**, are not photoreactive *per se*, whereas the benzoylMD probes **1**–**3** are. (C) AfBPP strategy: this approach aims at identifying proteins that interact with the PD-AfBPP drug metabolite in living parasites incubated with a parent precursor designed as (*pro*-) PD-AfBPP. The PD-AfBPP probe is released from the (*pro*-) PD-AfBPP probe through benzylic oxidation upon bioactivation in the living cell or following UV irradiation. Upon UV irradiation, covalent crosslinking of PD-AfBPP to its potential targets in yeast and *P. falciparum* proteomes occurs and enrichment of the probe-protein-biotin adducts is achieved by a CuAAC reaction between the probe-derived alkyne and the biotin azide. After streptavidin pulldown, enriched proteins are digested on-beads, and tryptic peptides identified by label-free quantitative mass spectrometry (LFQ) using LC–MS/MS.

es S5–S8). To the best of our knowledge, the use of tetrakis (acetonitrile) copper (I) with bathocuproinedisulfonic acid (BCDA) ligand has never been used before in ABPP/AfBPP experiments to catalyze the CuAAC reaction under aqueous conditions. It gave excellent results in our hands and the highest yield (85 %) was reached using the following conditions:

24 μM probe (0.5% ACN in PBS), 300 μM Cu(I):BCDA, 50 μM biotin-PEG3-azide, 0.3% SDS at 56 °C for 90 minutes under anaerobic conditions.

Design and Synthesis of Optimized Photoreactive 'Clickable' 3-benz (o)ylmenadiones

The workflow AfBPP methodology was effective on large amounts of purified recombinant protein, and we expected the same to be true when the probe is incubated with a complex protein mixture. However, this was not the case, likely due to the low yield of the UV crosslinking step (~5%)[19] Hence, we decided to first improve the photoreactivity of probe **1** by introducing a fluorine atom in C-6, leading to the 6-fluoro-benzoylMD-alkyne (probe **3**), to increase the benzoylMD photo-reduction efficacy.

Using the synthetic route to prepare the benzoylMD probe **1**, originally described in ref. [19], we synthesized the new 3-benzyl- and 3-benzoylMD alkyne probes **5** and **3** bearing a fluorine atom at the position **6** of the naphthoquinone (See supporting information, section A including Scheme S1). The only modification to the synthesis pathway comes from the use of the 6-fluoro-menadione, as starting material, that was prepared in 6 steps in a high-yielding sequence recently described,[24] as starting material instead of the commercial menadione. Of note, in this work, the **6-fluoro-PDO** could also be obtained from the **6-fluoro-PD** using a photoredox reaction under UV light and in the presence of dioxygen to oxidize the benzylic position of the benzylMD leading to **6-fluoro-PDO** with 37% overall yield (2 steps).

Electrochemistry Characterization

Herein, we briefly describe the electrochemistry data acquired on the different probes synthesized in this work (See supporting information, Table S2 and Figures S9–S16). We compared the redox properties of the 6-H and 6-fluorinated benzylMDs. The typical electrochemical profiles of benz(o)ylMD[17,25] and menadione analogues[26] (2-methyl-1,4-naphthoquinone, NQ) have been already described and discussed in detail in previous studies. They rely on two consecutive one-electron reversible waves, which correspond to the sequential NQ core reduction leading to the semi-NQ and dihydro-NQ, respectively. For benzoylMDs (probes **1**–**3**, **PDO**, **6-fluoro-PDO**) a third weak and broad wave is observed at much more negative values and is attributed to redox process centered on the benzoyl carbonyl unit (See supporting information, Figures S11–S16). In the absence of the carbonyl group, the new benzylMD derivatives with an alkyne group in *para*, e.g. probe **4**, are significantly less oxidant compared to their benzoylMD congeners, as observed for **PD** vs **PDO**[17] and **4** vs **1**, making the reduction of semi-NQ to dihydro-NQ more difficult (See supporting information, Table S2). In the case of the benzoylMD, the substitution with an alkyne moiety has a significant effect on the redox process centered on the carbonyl function, without profoundly altering the redox properties centered on the NQ moiety. A difference of about 50 mV between the alkyne and trifluoromethyl group substituted in C-4' of the benzoylMDs (**1** vs **PDO**) is indeed detected, suggesting that the alkyne unit favors the carbonyl reduction. In probe **3**, both combined substitutions – a fluorine atom at C-6 of the menadione core and a *para*-alkyne function on its benzyl moiety – favor the reduction of the semi-NQ and the carbonyl function, an effect which was expected to improve the photo-crosslinking properties in an AfBPP application.

Optimization of the Photoaffinity Labeling of GSH with Probe 3

The photolabeling properties of probe **3** were tested in comparison to former probes **1**–**2**, and confirmed to provide better yield of reaction (13% in the best condition vs. 5%,[19] See supporting information, Figure S17). The photolabeling was then investigated in the AfBPP conditions procedure, with 10% ACN, but gave poor yield results. Therefore, we introduced propan-2-ol as co-solvent. This solvent was already used in the benzophenone-like UV-irradiation reaction to favor radical triplet excited state formation.[27,28] The generated biradicaloid triplet excited state lifetime of the benzophenone is shorter in the presence of propan-2-ol than in other organic solvents. This can be very useful to avoid nonspecific labeling, especially when the probe interacts weakly with its target.[21] In the newly optimized conditions, the photolabeling reaction was carried out in a final percentage of 10% propan-2-ol and 10 μM probe **3** for 15 minutes of irradiation, yielding to 21% adduct (See supporting information, Figure S18).

Proteome Analysis of *S. cerevisiae*

We previously demonstrated that **PD** inhibits yeast respiratory growth and that the mitochondrial respiratory chain flavoprotein NADH-dehydrogenases play a key role in **PD** activity.[29] The deletion of the *NDE1* gene encoding the main NADH-dehydrogenase in yeast resulted in a decreased sensitivity to **PD**.[29] Before performing an AfBPP analysis on this model organism, we first performed a label-free quantitative proteomic study to evaluate the depth of our proteomic set up (1556 proteins representing 26% of the yeast open reading frames) as well as the effects of *NDE1* gene deletion (See supporting information, Figure S19).

Affinity-Based Protein Profiling on *S. cerevisiae* Protein Extracts

We performed AfBPP on yeast using the optimized conditions. WT yeast cells were lysed and the protein extract quantified. For each condition, 400 μg were incubated with 10 μM probe **3**, or ACN (used as control), in the presence of 10% propan-2-ol, with irradiation at 350 nm over 15 minutes to cross link the probe to target proteins. The protein extracts were then

subjected to the click reaction to biotinylate the clickable drug bound to the protein targets. After the click reaction, the sample was incubated with streptavidin beads, and the bound proteins were directly digested on beads. The peptide mixture was analyzed by nanoLC-MS/MS. Of the 875 proteins identified (Supplementary Table S2), roughly 500 proteins per replicate were quantified after stringent filtering (Figure 2, Panels A–B). Among these, 11 were found to be statistically more abundant in the AfBPP experiments than in the controls, given an FDR of less than 5% (Supplementary Table S3). Of these 11 proteins, 3 are involved in oxidoreductase activities (Pdb1, Dot5, Scs7) and one belongs to the yeast flavoproteome (Pdx3).[30] Interestingly Pdx3 is localized in the mitochondria and we previously showed that mitochondrial flavoenzymes played a key role in the activity of PD.[31] Pdb1 is the E1 beta subunit of the pyruvate dehydrogenase complex (PDH) also localized in the mitochondria. In addition to E1, PDH is formed of E2 (dihydrolipoamide acetyltransferase) and E3 (dihydrolipoamide dehydrogenase) components, with the structural protein Pdx1. We previously found that E3 (or Lpd1) and Lip2, acting in the attachment of lipoic acid groups to E2 were involved in PD activity.[31] The role of Pdb1 will be worth investigating. Dot5 and Scs7 are localized to the nucleus and the endoplasmic reticulum, respectively, but they might also be interesting to analyze.

Antimalarial Properties and Localization of (*pro*-) AfBPP Probes

Before performing AfBPP on *P. falciparum*, we first validated that the (*pro*-) AfBPP probes were active on parasites. **PD**, its 6-fluoro analogue **6-fluoro-PD**,[32] and probe **1**[19] are equally active against the CQ-resistant Dd2 strain with similar IC_{50} values. Probe **5** is also effective against *P. falciparum*, although less than **PD**, with IC_{50} values of 179.2 ± 27.2 nM and 46.6 ± 21.2 nM, respectively, on the drug sensitive strain NF54. As previously observed in both parasites[15,33] and yeast,[29,33] and despite being the key metabolites of benzylMDs,[20] benzoylMDs like probe **3** (the putative metabolite of probe **5**), do not display a high antimalarial activity, with IC_{50} of *ca.* 10–50 fold higher than those of the corresponding benzylMD. This can be explained by the poor internalization of benzoylMD metabolites in pRBCs or yeast when given to live cells. We further demonstrated that probe **5** was efficiently internalized into parasites. For this, parasites at the young trophozoite stage were incubated with probe **5**, or no probe as control, for 2 and 4 h before fixation. Probe **5** was labeled with a fluorescent probe carrying an azide function (Alexa Fluor 488) through a click reaction (Figure 3). After 2 h or 4 h of incubation, probe **5** presented a general but heterogeneous distribution inside parasites, suggesting that it may be specifically concentrated in or around certain organelles. We therefore performed co-staining with antibodies against proteins that are specific to mitochondria and apicoplast (Figure 3). We observed an

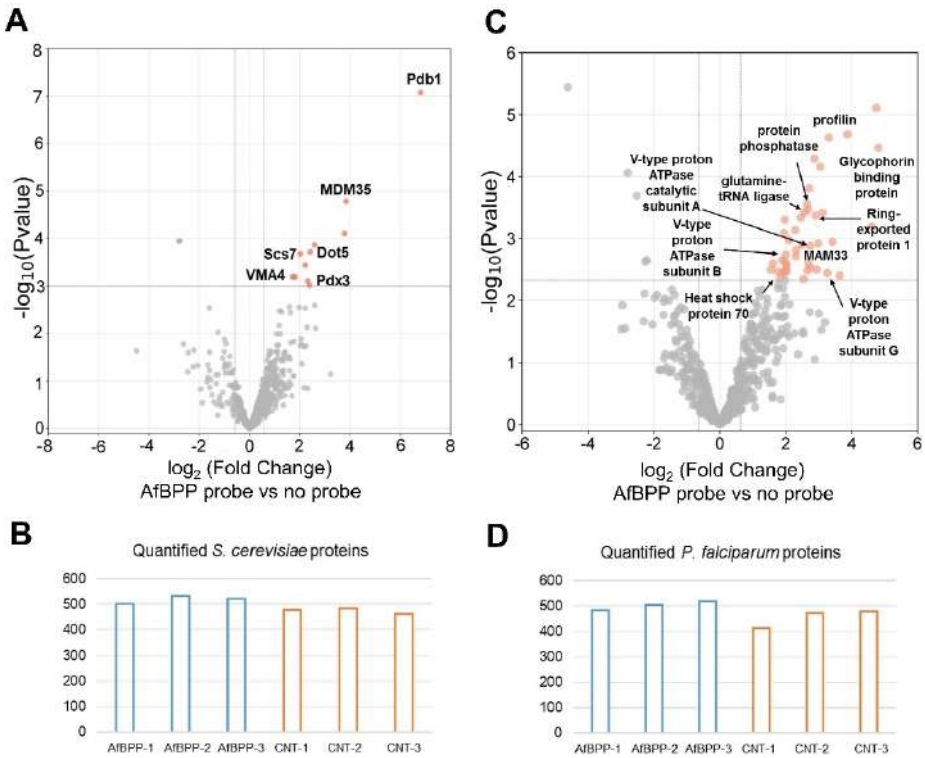

Figure 2. Volcano plots A and C represent *S. cerevisiae* proteins quantified in the AfBPP (AfBPP-1 to −3) *versus* control (CNT-1 to 3) experiments with probe **3**, and *P. falciparum* proteins quantified in the AfBPP (AfBPP-1 to −3) versus control (CNT-1 to −3) experiments with probe **5**, respectively. The red dots correspond to significantly enriched proteins in AfBPP samples. Panels B and D show the number of quantified proteins by replicate after stringent filtering for *S. cerevisiae* and *P. falciparum* respectively.

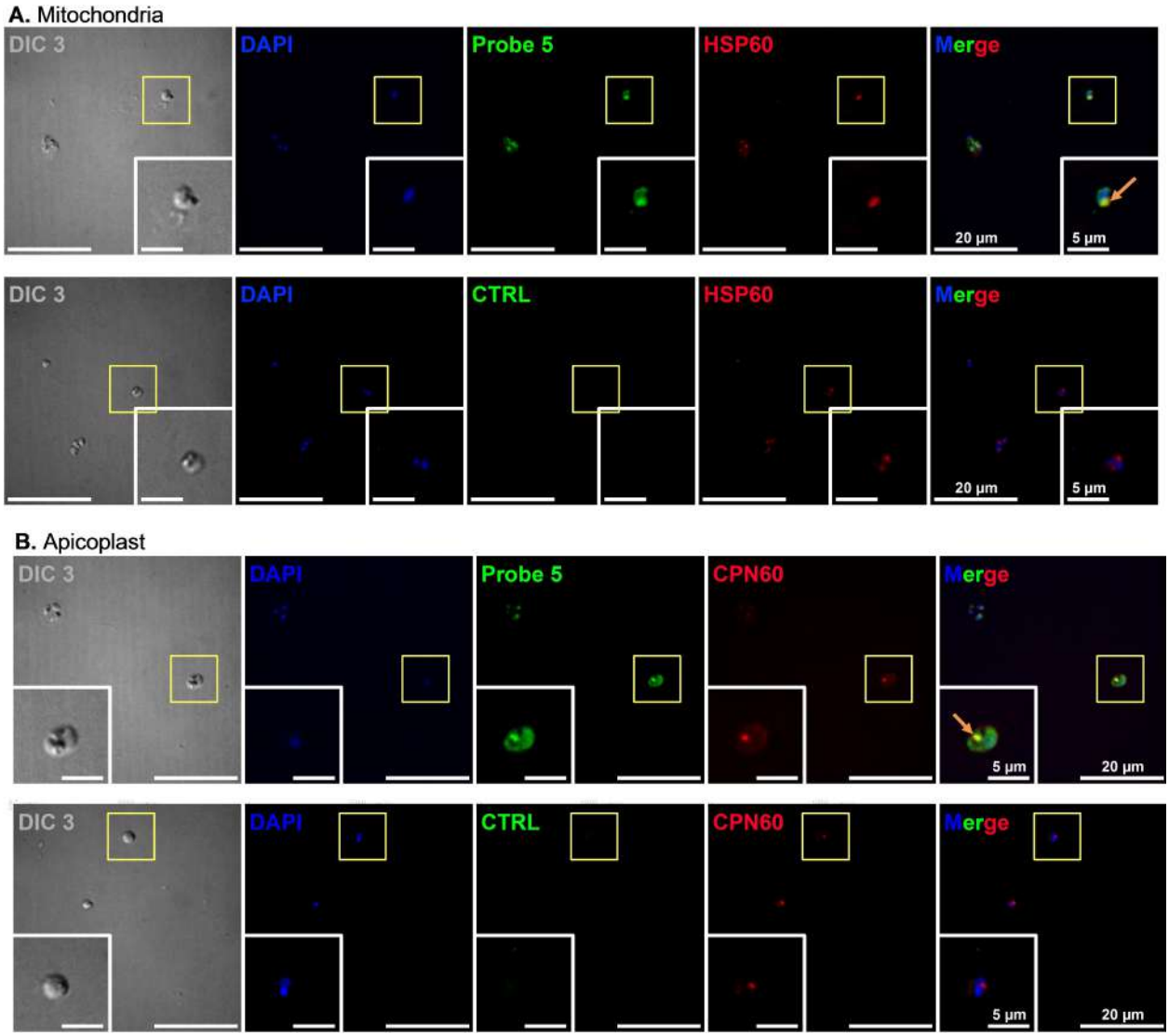

Figure 3. Cellular localization of probe **5** in asexual blood stages of *P. falciparum* (trophozoite stage) after 2 h of incubation. The probe was detected using CuAAC reaction with Alexa Fluor 488-azide (green). Nucleic acids were DAPI-stained (blue), and antibodies specific to *P. falciparum* HSP60 and CPN60 were used to localize the mitochondria (panel A, red) and the apicoplast (panel B, red), respectively. Controls were incubated without drugs. Data from 3 replicates.

association of probe **5** and apicoplast or mitochondria signals in 32% and 48% of the parasites, respectively. This association did not appear to depend on the age of the parasite. The presence of probe **5** inside parasites, and its antimalarial activity indicated that we could use it as a (*pro*-) AfBPP probe to identify putative benzylMD targets in *P. falciparum*.

Affinity-Based Protein Profiling on *P. falciparum* Parasites

To perform the AfBPP in *P. falciparum*, and because of very limited material available at early stages, we incubated pRBCs (NF54 strain) at 24 h post invasion (young trophozoite stage) with 5 µM of (*pro*-) AfBPP probe **5**, or with 0.08% DMSO as control. pRBCs were lysed after 5 h of treatment, and the parasites washed to remove the excess of hemoglobin. Parasite pellets were then irradiated for 15 min and lysed, and protein extracts were subjected to click chemistry and pulldown according to our optimized protocol. The peptide mixture was analyzed by nanoLC-MS/MS. Proteins were identified using the *P. falciparum* NF54 proteome from the PlasmoDB database. Of the 960 proteins identified (Supplementary Table S4), roughly 500 proteins per replicate were quantified after stringent filtering (Figure 2, Panels C–D). Among these, 44 were found to be statistically more abundant in the AfBPP experiments than in the controls without probe, given an FDR of less than 5% (Supplementary Table S5).

We analyzed the localization and putative function of the 44 proteins (Supplementary Table S6). The list did not appear to be enriched in proteins from a specific subcellular organelle, which is in accordance with the general albeit heterogeneous localization of probe **5** (Figure 3). Of note, and although benzylMDs are expected to be activated by and to redox cycle with flavoenzymes, there was none in the list of enriched

proteins in probe **5** samples. Still, we noted the presence of 3 subunits of the parasitic V-type proton ATPase, a complex that was also identified in the AfBPP experiment performed in yeast (VMA4). In *P. falciparum* trophozoites, the V-type proton ATPase controls the pH of the parasite cytosol and food vacuole.[34] Exposure of malarial parasites to oxidative stress triggers a drop in the intracellular ATP level and inhibits V-type H(+)-ATPase, causing a loss of pH control in both the parasite cytosol and the internal digestive vacuole.[35] Furthermore, the antimalarial ROS-inducer plakortin was reported to generate protein modifications at ring and trophozoite stages, by triggering lipid peroxidation and formation of 4-HNE-protein conjugates in pRBC with the V-type proton ATPase catalytic subunit A and heat shock protein Hsp70–1,[36] that was also pulled down with the AfBPP probe. The most enriched proteins in probe **5** samples are all essential for the parasite life cycle: a glycophorin binding protein (surface protein), 2 mitochondrial chaperonins, and profilin (cytoplasmic). It will be interesting to evaluate the contribution of some of these candidate genes in the MoA of benzylMDs, and to further identify putative **PD** target proteins, varying exposure time and exploring other parasite stages, notably rings that are especially sensitive to benzylMDs, and gametocytes.

Conclusions

The yeast and *P. falciparum* protein profiling data generated in the presence of **PD** affinity-based probes built on the 3-benz (o) ylmenadione motif are presented here in this first special issue "Chemical Biology *Tour de France*". After a first proof-of-concept with a pure recombinant protein,[19] yeast or plasmodial lysates were photoirradiated with new AfBPP or (*pro*-) AfBPP probes, and the proteins were pulled-down after a CuAAC reaction with BA, allowing us to evaluate the reactivity of the new probes in a MS-based target analysis. We demonstrated that (*pro*-) AfBPP probes are indeed suitable for the search and exploration of **PD** target proteins.

Altogether, these experiments not only represent a "*Tour de force*" in the field of chemical biology and probe design for antimalarial drugs, but also showcase how to approach such challenging tasks as target identification – which extends very generally to medicinal chemistry. Further optimization of the AfBPP probes and photoaffinity reaction conditions will be key in the future to investigate other *P. falciparum* stages with more limited material, notably rings and gametocytes, and various parasite strains expressing distinct degrees of susceptibilities to artemisinin.

Experimental Section

Chemistry. General

All the reagents and solvents were purchased from commercial sources and used as received, unless otherwise stated. The ^{1}H and ^{13}C NMR spectra were obtained in $CDCl_3$ as solvents using a 400 MHz or a 500 MHz spectrometer. Chemical shifts were reported in parts per million (δ). ^{1}H NMR data were reported as follows: chemical shift (δ ppm) (multiplicity, coupling constant (Hz), and integration). Multiplicities are reported as follows: s = singlet, d = doublet, t = triplet, q = quartet, m = multiplet, or combinations thereof. High-resolution mass spectroscopy (HRMS) spectra were recorded using the electron spray ionization (ESI) technique.

Chemistry. Synthesis of Precursors

Reactants and building blocks were purchased from commercial sources, such as Fluorochem, Sigma-Aldrich, BLDpharmtech or Alfa Aesar. 1,4-dimethoxy-2-methyl-naphthalene **7** was synthesized according to the previously published method.[37] **Synthesis of probes 1–5, 6-fluoro-PDO**. Synthetic processes and chemical analyses were detailed in the supporting information (Scheme S1 and section B1).

Peptide Photolabeling under UV Irradiation

Photolabeling of the GSH peptide with the probe **3** was performed under UV-irradiation with a 350 nm light generated by eight RPR-3500 A lamps of 200 W with a Rayonet photochemical reactor for different times at 16 °C. Stock solutions of GSH (Sigma) were prepared in PBS 1×, instead, stock solutions of probe **3** were prepared in ACN. In all the reactions GSH and probe **3** stock solutions were deoxygenated separately and then mixed to start the photoreaction. Samples were deoxygenated by five alternative cycles of vacuum and argon flux in anaerobic vials, longer argon than vacuum cycles were used to avoid ACN evaporation. The different concentration of the probe and the GSH peptide used for the experiment were incubated and then irradiated for the specific time. After irradiation 1 nmol of each sample was analyzed by LC–MS with a Q-TOF mass spectrometer (maXis II, Bruker) coupled with an Agilent 1100 series LC. Samples were separated on an XBridge Peptide BEH (Waters) C18 column (300 Å, 3.5 μm, 2.1 mm×250 mm) column working at a 250 μL/min flow rate, using a non-linear 5–95% gradient of eluent B (0.08% TFA, in ACN LC–MS Grade) over 40 min.

Click Reaction Optimization in Aqueous Cconditions

The CuAAC was optimized by tuning several conditions in terms of probe solvent, reaction temperature, copper complex catalyst (see Table 1). The reactions under anaerobic conditions were carried out as previously reported.[19] The Cu(I) complex catalyst (See supporting information, Table S1) was prepared by mixing bathocuproin sulfonate disodium salt hydrate (BCDA, ThermoFisher) and tetrakis (acetonitrile) copper (I) (BLD Pharmatech Gmb, Germany) under anaerobic conditions. Each reaction was carried out in the presence of 0.3% sodium dodecyl sulfate (SDS) final concentrations. The reactions were monitored over time and the products analyzed by LC-UV-MS with a Q-ToF (maXis II, Bruker) mass spectrometer coupled to an HPLC and DAD detector (Agilent). Samples were fractionated with an XBridge Peptide BEH C18 column (300 Å, 3.5 μm, 2.1 mm×250 mm) column working at a 250 μL/min flow rate, using a non-linear 20–95% gradient of eluent B (0.08% TFA, in ACN LC–MS Grade) over 40 min. To calculate the yield of the reactions at each time, the peak areas of the extracted ion chromatogram (EIC) were used.

S. cerevisiae Cultures

The *S. cerevisiae* strains used were AD-9, referred as wild-type (WT) and its derived mutant Δ*NDE1* in which the gene encoding for the

protein Nde1 was deleted.[29] The cells were grown at 28 °C in a galactose medium (YPGal, yeast extract 1%, peptone 2%, galactose 2%, glucose 0.1%) and the culture was stopped at $OD_{600} \approx 2.5$.

Proteomic Analysis of *S. cerevisiae* Cells

The yeast pellets were lysed by adding 1 mL of RIPA buffer to ≈200 mg of pellet. The resuspended pellets were subjected to 10 cycles of sonication (1 cycle = 30 sec sonication on and 30 sec off) at 4 °C. The protein extracts were recovered by centrifugation at 16,000 g for 2 minutes at 25 °C. Triplicates of 50 μg of each lysate were subjected to enzymatic digestion with trypsin/LysC by using the single-pot, solid-phase-enhanced sample-preparation (SP3) technology. The peptide mixtures obtained were analyzed by nanoLC-MS/MS, the method is described below in the LC–MS/MS analysis part. The raw data obtained from the three wild-type and mutant samples were processed by MaxQuant for protein identification and quantification. Protein identification and quantification were performed with the software MaxQuant by using the UniProt database for *S. cerevisiae*. MaxQuant parameters for protein identification were set to 3 peptides at least, with 1% false discovery rate (FDR) confidence. We used Perseus software to perform the statistical analysis of the differentially expressed proteins. In particular, contaminants and reverse proteins were removed, proteins with 50% of valid values in at least WT or mutant group were retained for the following analysis. To obtain the differentially expressed proteins, a Student's t-test was performed fixing a 5% FDR (Benjamini-Hochberg adjusted p-value).

AfBPP Strategy on Recombinant PfGR and Western Blot Analysis

PfGR (200 μg) was incubated with 10 μM probe **2** and then photo-irradiated at 350 nm for 10 minutes at 16 °C. As control *PfGR* was incubated also with 0.5% ACN, in the absence of the probe. The click reaction was performed as described in the section 'Click reaction optimization in aqueous conditions', but adding an excess of 10× BA (Lumiprobe). The reaction mixture was precipitated by a classical methanol/chloroform procedure to remove the excess of unreacted species. The samples were resuspended in 200 μl of 150 mM NaCl, 0.1% NP-40 in PBS and incubated over-night at 4 °C with Pierce Streptavidin magnetic beads (10 μl), previously washed 5 times with the same buffer. The beads were washed one time with 300 mM NaCl in PBS, two times with 0.1% SDS in PBS, and, finally, with PBS. The biotinylated protein was eluted by adding Laemli buffer and incubating 10 minutes at 95 °C. The samples were loaded onto a 10% SDS-PAGE gel and then transferred onto a nitrocellulose membrane by means of Trans-Blot Turbo Transfer System (Bio-Rad). The membrane was blocked with 5% BSA in TBS, and then incubated over-night with 1:10,000 anti-biotin polyclonal antibody (ThermoFisher, cat. code #31852). Anti-Goat HRP antibody (ThermoFisher) incubation followed in 1:10,000 ratio for 45 minutes. The chemiluminescence signal was acquired after reaction with ECL substrate with ChemiDoc Touch Imaging System.

Affinity-Based Protein Profiling Procedure on *S. cerevisiae*

Yeast cells (AD1-9, WT) were lysed by overnight pellet incubation with lysis buffer (1% NP40, 150 NaCl, 1× PBS and protease inhibitors) and then by sonicating them 10 cycles (one cycles: 5 seconds sonication at 10% amplitude and 15 seconds on ice), then centrifuged for 10 minutes at 13,000 rpm at 4 °C. Protein extract was recovered and quantified (Pierce Assay 660 nm kit, Thermo Fisher) before to the deoxygenation protocol. Afterwards, protein extract was incubated for 15 minutes in triplicate with deoxygenated solution of the AfBPP probe **3** at 10 μM and 10% propan-2-ol (or ACN) used as control. The samples were then irradiated with an UV lamp at 350 nm for 15 minutes at 16 °C. All the solutions were subjected to click reaction, by adding a molar excess of 25 times of BA in 300 μM Cu:BCDA solution under deoxygenated conditions over 90 minutes at 56 °C. Reactions were stopped by adding EDTA in a final concentration of 5 mM and by buffer exchange protocol by using Zeba spin cartridges (Thermo Fisher) by using 0.2% NP40, 150 mM NaCl, 1× PBS. The samples were then incubated overnight at 4 °C with Streptavidin beads pre-washed with the same buffer used for the exchange protocol. The next day, the beads were washed 4 times (0.2% NP40, 300 mM NaCl, 1× PBS (1×); 0.1% SDS (2×); 1× PBS (1×)) and then incubated with a solution of DDT 5 mM in ammonium bicarbonate 50 mM for 30 minutes at 37 °C. A final concentration of 20 mM IAM in 50 mM ammonium bicarbonate was then added and the samples incubated for 30 minutes at 25 °C in the dark. The beads were washed once with 50 mM ammonium bicarbonate and then incubated with 1:10 w/w trypsin/lys-C (Promega) solution in 50 mM ammonium bicarbonate at 37 °C overnight. Peptides were eluted by washing the beads with ammonium bicarbonate, then dried and the peptide concentration was determined (Pierce™ Quantitative Peptide Assays & Standards, Product cat. code: #23275). The peptide mixtures were then subjected to a solid phase extraction (SPE) protocol using Oasis HBL 30 mg cartridges (Waters) and injected into an Orbitrap-Q Exactive Plus instrument, as reported in the "LC–MS/MS analysis" section, and data interpretation is reported in data analysis part.

In Vitro Anti-Plasmodium Activity Assays

The inhibition of intraerythrocytic parasite development by benzylMD derivatives and control agents (IC_{50} **PD** = 46.6 ± 21.2 nM) was determined in microtiter tests according to standard protocols. The *in vitro* antimalarial activity is expressed as 50% inhibitory concentration (IC_{50}). For this, *P. falciparum* wild-type strain NF54 was cultured at 37 °C in RPMI medium containing 5% human serum + 0.5% albumax and type A erythrocytes at a hematocrit of 3% under a low-oxygen atmosphere (5% CO_2, 5% O_2, 90% N_2) and 95% humidity following standard protocols.[38] These culture conditions were used for all *P. falciparum* experiments. Synchronous ring stage parasites (0–3 hpi) were obtained by centrifugation on a 75% percoll density centrifugation followed by 5% sorbitol treatment.[39] Inhibitors were dissolved at 6 mM in 100% DMSO, diluted in culture medium and added at decreasing concentrations (1/3 serial dilutions in duplicates) to synchronized ring stage parasite cultures in microtiter plates (0.5% parasitemia, 1.5% hematocrit) and incubated for 72 h. The final inhibitor concentrations in each assay ranged from 1.4 nM to 3 μM. Growth inhibition was determined in a SYBR green assay as described previously.[40,41] Experiments were performed at least three times independently.

Bioimaging of *(pro-)* AfBPP Probe 5 in *P. falciparum* Trophozoites

Trophozoite stages of *Plasmodium falciparum* NF54 strain (5% parasitemia, 1.5% hematocrit) were incubated with probe **5** at 10 μM for 2 or 4 hours. Dual Click chemistry and immuno-staining were performed on fixed blood smear according to the described protocol[42] with some modifications. In brief, thin blood smears were fixed with 4% (w/v) paraformaldehyde in PBS and permeabilized for 10 min with 0.1% Triton X-100 in PBS. The click reaction was then performed for 30 minutes at room temperature with 5 μM of Alexa Fluor 488 Azide (Thermo Fisher, ref A10266) in the presence of $CuSO_4$ in the "Click-it" Cell Reaction Buffer Kit (Thermo Fisher, ref C10269) according to manufacturer's conditions. The

samples were then processed for co-staining with the mitochondria and apicoplast specific antibodies as follows. The slides were blocked with 3% (w/v) BSA in PBS for 15 minutes and incubated either with (1) mouse polyclonal antibodies raised against the mitochondrial protein *Pf*HSP60 (1:500 dilution in 3% BSA) (kind gift of Philippe Grellier, Muséum National d'Histoire Naturelle, Paris) followed by goat anti-mouse IgG conjugated with Alexa Fluor 647 (1:1000 dilution in 3% BSA) (Thermo Fisher, ref A21235), or with (2) rabbit polyclonal antibodies raised against *Toxoplasma gondii* CPN60 (1:500 dilution in 3% BSA, cross-reacting with *Pf*CPN60)[43] followed by goat anti-rabbit IgG conjugated with Alexa Fluor 647 (1:1000 dilution in 3% BSA) (Thermo Fisher, ref A21244). Parasite nuclei were stained with DAPI (1:1000 dilution in PBS) (Thermo Fisher, ref 62248). The slides were mounted in Immu-Mount (Epredia, ref 9990402) and image acquisition (z-series) was realized on a Zeiss axio observer Z1 inverse microscope equipped with a CSU–X1 Yokogawa spinning disk and an EMCCD camera Roper Evolve, and using a Plan apochromat 100×/1.40 oil objective. Images were processed with Fiji software (ImageJ2, version 2.14.0/1.54f) and final figures were compiled using the Quickfigures plugin. The images presented correspond to the sum of intensity projection of the z-series.

Affinity-Based Protein Profiling Procedure on *P. falciparum*

The *in-situ* AfBPP procedure closely follows the methodology outlined by Nardella and coworkers.[44] with some modifications. Tightly synchronized trophozoites stage parasite culture was obtained by subjecting late-stage schizont parasites to a 75% Percoll density centrifugation, followed by the collection of 0–3 hpi young newly formed rings with 5% sorbitol treatment. Parasites were then further cultured for 24 h. Highly synchronized trophozoites of *P. falciparum NF54* cultures (5% parasitemia and 3% hematocrit, 25 mL culture each) were treated with 5 μM of the (*pro*-) AfBPP probe **5** or 0.08% DMSO for a duration of 5 h. All treatments were carried out in triplicate. Subsequently, parasites were harvested by saponin lysis (using 0.15% saponin in ice-cold 1X PBS) and thoroughly washed in ice-cold 1X PBS to eliminate hemoglobin contaminants. Parasite pellets were resuspended in 1 mL of 1X PBS and transferred to glass tube compatible with photo-irradiation. They were exposed to a 15-minute irradiation at 350 nm on ice using a UV lamp. Parasite were then centrifuged and incubated for 5 minutes in 100 μL lysis buffer (PBS 1×, 1% SDS, 1 mM dithiothreitol (DTT) protease inhibitors cocktail), subjected to three cycle of freeze (−80 °C, 5 min)/thaw (42 °C, 2 min), sonicated 10 times for 5 seconds at 10% amplitude and centrifuged for 10 minutes at 13000 rpm at 4 °C. The protein extracts were quantified and for each condition, 300 μg were subjected to the click reaction by adding BA in a final concentration of 1 mM in 300 μM Cu:BCDA solution in deoxygenated conditions for 90 minutes at 56 °C. Reactions were stopped by adding EDTA to a final concentration of 5 mM and processed as for the yeast AfBPP protocol previously described.

LC–MS/MS Analysis

NanoLC-MS/MS analyses were performed with a nanoAcquity UPLC device (WatersCorporation, Milford, MA, USA) coupled to a Q-Exactive Plus mass spectrometer (ThermoFisher Scientific, Waltham, MA, USA). Peptide separation was performed on an Acquity UPLC BEH130 C18 column (250 mm×75 μm with 1.7-μm-diameter particles) and a Symmetry C18 precolumn (20 mm×180 μm with 5-μm-diameter particles, Waters). The solvent system consisted of 0.1% formic acid (FA) in water and 0.1% FA in ACN starting from 1% to 35% of eluent B over 79 minutes. The system was operated in data dependent acquisition mode with automatic switching between MS and MS/MS modes. The ten most abundant ions were selected on each MS spectrum for further isolation on a scan ranging from 300 to 1800 m/z. HCD fragmentation method was used with a collision energy (NCE) set to 27. The dynamic exclusion time was set to 60 sec.

Data Analysis

Raw data files were uploaded in MS Angel software and peptide quantification performed with MASCOT interface by using the following parameters: "trypsin" as enzyme with at least one missed cleavage, "carbamidomethyl" as a fixed modification, "oxidation of Met" as variable modifications, 0.05 Da as MS/MS tolerance, and 5 ppm as peptide tolerance. Specific databases were used for the protein identification, the Uniprot database for *S. cerevisiae* and PlasmoDB database for the *P. falciparum* NF54 strain (sequence protein fasta file release number 66). Results were then imported into Proline software (http://proline.profiproteomics.fr)[45] to validate (1% FDR at PSM and protein level) and quantify the protein identified. Prostar software was used for the statistical analysis.[46]

To be considered, proteins must be identified in all 3 replicates in at least one condition. Protein abundances were normalized using 0.15% quantile centering overall. Imputation of missing values was done using the approximation of the lower limit of quantification by the 2.5% lower quantile of each replicate intensity distribution ("det quantile"). A Limma moderated t-test was applied on the dataset to perform differential analysis. p-Values calibration was corrected using adapted Benjamini-Hochsberg method[47,48] and False Discovery Rate was optimized for each pairwise comparison.

Supporting Information

Pages S2–S3: A. Synthetic Procedures (including Scheme S1); Pages S3–S7: B1. Characterization of Compounds & Materials; Pages S7–S12: B2.1. Characterization of the photo-crosslinked and probe-reacted protein adducts (including Figures S1–S4); Page S13–S15: B2.2. Optimization of the click reaction with probes 1–3 (including Table S1 and Figures S5–S7); Page S16: B2.3. Detection of the photo-crosslinked PfGR and the protein-probe 2-adducts by Western-blot and Immunofluorescence (including Figure S8); Pages S17–S21: B2.4. Electrochemistry (including Table S2 and Figures S9–S16); Pages S22–S23: B2.5. Optimization of the peptide GSH photolabeling in the presence of new probe 3 (including Figures S17–S18); Page S24: B2.6. Proteome analysis of S. cerevisiae strains by MS analysis (including Figure S19); Page S24: C. Data Deposition; Pages S25–S42: 1H, 19F, and 13 C {1H} NMR spectra of all new compounds.

Supplementary Tables: S1–S6. Data are available via ProteomeXchange with identifier PXD050982.

Abbreviations

ACN	acetonitrile
AfBPP	affinity-based protein profiling
BA	biotin azide
BCDA	Bathocuproinedisulfonic acid

benzoylMD	3-benzoylmenadione
benzylMD	3-benzylmenadione
β-met	β-mercaptoethanol
CHX	cyclohexane
CuAAC	copper (I)-catalyzed alkyne-azide cycloaddition
DCM	dichloromethane
EIC	extracted ion chromatogram
FA	formic acid
FDR	false discovery rate
GSH	glutathione
ESIPT	excited state intramolecular photoinduced transfer
LFQ	label-free differential quantitative
MoA	mode of action
PD	plasmodione
PDO	plasmodione oxide
pRBC	parasitized red blood cells
TCEP	Tris (2-carboxyethyl) phosphine
T	toluene

Acknowledgements

E. D.-C. and S. A. B. wish to thank the Laboratoire d'Excellence (LabEx) ParaFrap [ANR-11-LABX-0024], for funding, providing B. D.'s PhD salary, and for initiating and fostering this scientific research and collaboration. This work was also supported by the European Campus EUCOR, via the seed-money program ("ROSkillers" project), Région Grand'Est program "Compétences Recherche Jeunes Chercheurs – Attractivité Année 2022" with the project "plasmo.Fish&Click" and for the postdoc salary to I. I. This work was further funded by grants from CNRS Mission pour les initiatives transverses et interdisciplinaires (MITI "Vie & Lumière" program, grant to E. D.-C., S. A. B. and C. S.), from the ANR-FNS (ANR-22-CE93-0005-01, "ROS Action" project to E. D–C., B. M. and S. A. B.). V. M.'s 6 month-training in Strasbourg was supported by the University of Naples (PhD salary) and a STSM grant from the COST Action CA21111 "OneHealth.Drugs". E. D.-C. and B. D. thank Matthieu Roignant for the complete chemical analysis of compound 6-fluoro-1,4-dimethoxy-2-methylnaphthalene **11**. The French Proteomic Infrastructure (ProFI; ANR-10-INBS-08-03, FR2048) is acknowledged for its support to the MS-based proteomics analysis. R. K. is grateful to the IBMC Insectary platform and to Jean Daniel Fauny and Romain Vauchelle from the IBMC Microscopy Platform for their training and guidance in fluorescence microscopy. The laboratories also receive support from CNRS (E. D.-C., S. A. B., C. S. and B. M.), Inserm (S. A. B.) and from the University of Strasbourg (E. D.-C., S. A. B. and C. S.).

Conflict of Interests

The authors declare no conflict of interest.

Data Availability Statement

The data that support the findings of this study are available in the supplementary material of this article.

Keywords: Activity-Based Protein Profiling · Antiprotozoal agents · Biological Chemistry and Chemical Biology · Photoaffinity Labeling · Proteomics

[1] I. Iacobucci, V. Monaco, F. Cozzolino, M. Monti, *J. Proteomics* **2021**, *230*, 103990.
[2] F. Cozzolino, I. Iacobucci, V. Monaco, M. Monti, *J. Proteome Res.* **2021**, *20*, 3018.
[3] K. Lu, C. Mansfield, M. Fitzgerald, E. Derbyshire, *ChemBioChem* **2021**, *22*, 2591.
[4] Y. Gao, M. Ma, W. Li, X. Lei, *Adv. Sci.* **2023**, e2305608.
[5] M. Evans, B. Cravatt, *Chem. Rev.* **2006**, *106*, 3279.
[6] B. Cravatt, A. Wright, J. Kozarich, *Annu. Rev. Biochem.* **2008**, *77*, 383.
[7] A. Berger, P. Vitorino, M. Bogyo, *Am. J. PharmacoGenomics* **2004**, *4*, 371.
[8] M. Nodwell, S. Sieber, *Top. Curr. Chem.* **2012**, *324*, 1.
[9] L. Carvalho, G. Bernardes, *ChemMedChem.* **2022**, 17, e202200174.
[10] M. Bogyo, *Trends Parasitol.* **2023**, *39*, 83.
[11] H. Fang, B. Peng, S. Y. Ong, Q. Wu, L. Li, S. Q. Yao, *Chem. Sci.* **2021**, *12*, 8288.
[12] L. Wankyu, Z. Huang, C. W. Am Ende, U. Seneviratne, *STAR Protoc.* **2021**, *2*, 100593.
[13] R. Fuerst, R. Breinbauer, *ChemBioChem* **2021**, *22*, 630.
[14] L. Krammer, R. Breinbauer, *Isr. J. Chem.* **2023**, *63*, e202200086.
[15] T. Müller, L. Johann, B. Jannack, M. Brückner, D. Lanfranchi, H. Bauer, C. Sanchez, V. Yardley, C. Deregnaucourt, J. Schrével, M. Lanzer, R. Schirmer, E. Davioud-Charvet, *J. Am. Chem. Soc.* **2011**, *133*, 11557.
[16] K. Ehrhardt, C. Deregnaucourt, A. Goetz, T. Tzanova, B. Pradines, S. Adjalley, S. Blandin, D. Bagrel, M. Lanzer, E. Davioud-Charvet, *Antimicrob. Agents Chemother.* **2016**, *60*, 5146.
[17] P. Sidorov, I. Desta, M. Chessé, D. Horvath, G. Marcou, A. Varnek, E. Davioud-Charvet, M. Elhabiri, *ChemMedChem.* **2016**, *11*, 1339.
[18] M. Bielitza, D. Belorgey, K. Ehrhardt, L. Johann, D. Lanfranchi, V. Gallo, E. Schwarzer, F. Mohring, E. Jortzik, D. Williams, K. Becker, P. Arese, M. Elhabiri, E. Davioud-Charvet, *Antioxid. Redox Signaling* **2015**, *22*, 1337.
[19] B. Cichocki, V. Khobragade, M. Donzel, L. Cotos, S. Blandin, C. Schaeffer-Reiss, S. Cianférani, J. Strub, M. Elhabiri, E. Davioud-Charvet, *JACS Au* **2021**, *1*, 669.
[20] B. Cichocki, M. Donzel, K. Heimsch, M. Lesanavičius, L. Feng, E. Montagut, K. Becker, A. Aliverti, M. Elhabiri, N. Cenas, E. Davioud-Charvet, *ACS Infect. Dis.* **2021**, *7*, 1996.
[21] G. Dormán, H. Nakamura, A. Pulsipher, G. Prestwich, *Chem. Rev.* **2016**, *116*, 15284.
[22] E. Karaj, S. Sindi, L. Viranga Tillekeratne, *Bioorg. Med. Chem.* **2022**, *62*, 116721.
[23] N. Trometer, B. Cichocki, Q. Chevalier, J. Pécourneau, J. Strub, A. Hemmerlin, A. Specht, E. Davioud-Charvet, M. Elhabiri, *J. Org. Chem.* **2023**, *89*, 2104.
[24] N. Trometer, M. Roignant, E. Davioud-Charvet, *Org. Process Res. Dev.* **2022**, *26*, 1152.
[25] L. Cotos, M. Donzel, M. Elhabiri, E. Davioud-Charvet, *Chem. Eur. J.* **2020**, *26*, 3314.
[26] M. Elhabiri, P. Sidorov, E. Cesar-Rodo, G. Marcou, D. Lanfranchi, E. Davioud-Charvet, D. Horvath, A. Varnek, *Chemistry* **2015**, *21*, 3415.
[27] H. Görner, *J. Photochem. Photobiol.* **2011**, *224*, 135.
[28] K. Grzyb, R. Frański, T. Pedzinski, *J. Photochem. Photobiol. B* **2022**, *234*, 112536.
[29] P. Mounkoro, T. Michel, S. Blandin, M. Golinelli-Cohen, E. Davioud-Charvet, B. Meunier, *Free Radical Biol. Med.* **2019**, *141*, 269.
[30] V. Gudipati, K. Koch, W. Lienhart, P. Macheroux, *Biochim. Biophys. Acta* **2014**, *1844*, 535.
[31] P. Mounkoro, T. Michel, M. Golinelli-Cohen, S. Blandin, E. Davioud-Charvet, B. Meunier, *Free Radical Biol. Med.* **2021**, *162*, 533.
[32] E. Rodo, L. Feng, M. Jida, K. Ehrhardt, M. Bielitza, J. Boilevin, M. Lanzer, D. Williams, D. Lanfranchi, E. Davioud-Charvet, *Eur. J. Org. Chem.* **2016**, *11*, 1982.

[33] L. Feng, D. Lanfranchi, L. Cotos-Munoz, E. Cesar Rodo, K. Ehrhardt, A. Goetz, H. Zimmerman, F. Fenaille, S. Blandin, E. Davioud-Charvet, *Org. Biomol. Chem.* **2018**, *16*, 2647.
[34] M. Forgac, *Nat. Rev. Mol. Cell Biol.* **2007**, *8*, 917.
[35] D. Schalkwyk, K. Saliba, G. Biagini, P. Bray, K. Kirk, *PLoS One* **2013**, *8*, e58933.
[36] O. Skorokhod, D. Davalos-Schafler, V. Gallo, E. Valente, D. Ulliers, A. Notarpietro, G. Mandili, F. Novelli, M. Persico, O. Taglialatela-Scafati, P. Arese, E. Schwarzer, *Free Radical Biol. Med.* **2015**, *89*, 624.
[37] W. Friebolin, B. Jannack, N. Wenzel, J. Furrer, T. Oeser, C. Sanchez, M. Lanzer, V. Yardley, K. Becker, E. Davioud-Charvet, *J. Med. Chem.* **2008**, *51*, 1260.
[38] W. Trager, J. Jensen, *Science* **1976**, *193*, 673.
[39] C. Lambros, J. Vanderberg, *J. Parasitol.* **1979**, *65*, 418.
[40] M. Smilkstein, N. Sriwilaijaroen, J. Kelly, P. Wilairat, M. Riscoe, *Antimicrob. Agents Chemother.* **2004**, *48*, 180.
[41] D. Beez, C. Sanchez, W. Stein, M. Lanzer, *Antimicrob. Agents Chemother.* **2011**, *55*, 50.
[42] C. J. Tonkin, G. G. Van Dooren, T. P. Spurck, N. S. Struck, R. T. Good, E. Handman, A. F. Cowman, G. I. McFadden, *Mol. Biomol. Parasitol.* **2004**, *137*, 13.
[43] S. Agrawal, G. G. Van Dooren, W. L. Beatty, B. Striepen, *J. Biol. Chem.* **2009**, *284*, 33683.
[44] F. Nardella, I. Dobrescu, H. Hassan, F. Rodrigues, S. Thiberge, L. Mancio-Silva, A. Tafit, C. Jallet, V. Cadet-Daniel, S. Goussin, A. Lorthiois, Y. Menon, N. Molinier, D. Pechalrieu, C. Long, F. Sautel, M. Matondo, M. Duchateau, G. Médard, B. Witkowski, A. Scherf, L. Halby, P. Arimondo, *iScience* **2023**, *26*, 105940.
[45] D. Bouyssié, A. Hesse, E. Mouton-Barbosa, M. Rompais, C. Macron, C. Carapito, A. Gonzalez de Peredo, Y. Couté, V. Dupierris, A. Burel, J. Menetrey, A. Kalaitzakis, J. Poisat, A. Romdhani, O. Burlet-Schiltz, S. Cianférani, J. Garin, C. Bruley, *Bioinformatics* **2020**, *36*, 3148.
[46] S. Wieczorek, F. Combes, C. Lazar, Q. Giai Gianetto, L. Gatto, A. Dorffer, A. Hesse, Y. Couté, M. Ferro, C. Bruley, T. Burger, *Bioinformatics* **2017**, *33*, 135.
[47] Y. Benjamini, Y. Hochberg, *J. Royal Stat. Soc. Ser.* **1995**, *57*, 289.
[48] Y. Benjamini, Y. Hochberg, *J. Educ. Behav. Stat.* **2000**, *25*, 60.
[49] J. Cox, M. Mann, *Nat. Biotechnol.* **2008**, *26*, 1367.
[50] S. Tyanova, T. Temu, P. Sinitcyn, A. Carlson, M. Hein, T. Geiger, M. Mann, J. Cox, *Nat. Methods* **2016**, *13*, 731.
[51] E. W. Deutsch, N. Bandeira, Y. Perez-Riverol, V. Sharma, J. Carver, L. Mendoza, D. J. Kundu, S. Wang, C. Bandla, S. Kamatchinathan, S. Hewapathirana, B. Pullman, J. Wertz, Z. Sun, S. Kawano, S. Okuda, Y. Watanabe, B. MacLean, M. MacCoss, Y. Zhu, Y. Ishihama, J. A. Vizcaíno, *The ProteomeXchange Consortium at 10 years: 2023 update. Nucleic Acids Res.* **2023**, *51(D1)*, D1539–D1548.

Manuscript received: February 29, 2024
Revised manuscript received: April 16, 2024
Accepted manuscript online: April 19, 2024
Version of record online: May 28, 2024